Agronomy Research **16**(3), 758–768, 2018
https://doi.org/10.15159/AR.18.131

Using the FEM model for design the heat treatment of an agricultural tools

A. Kešner[1,*], R. Chotěborský[1], M. Linda[2] and M. Hromasová[2]

[1]Czech University of Life Sciences Prague, Faculty of Engineering, Department of Material Science and Manufacturing Technology, Kamýcká 129, CZ165 21 Prague, Czech Republic
[2]Czech University of Life Sciences Prague, Faculty of Engineering, Department of Eletrical Engineering and Automation, Kamýcká 129, CZ165 21 Prague, Czech Republic
[*]Correspondence: kesner@tf.czu.cz

Abstract. Agricultural tools need mechanical properties such as abrasive wear, hardness and toughness. These mechanical properties are achieved by choosing a suitable steel and subsequent heat treatment of the steel. Phases of the microstructure affects the final steel properties. The phase composition in the steel is influenced with the designing of the heat treatment. 25CrMo4 steel was investigated for the production of agricultural tools. The heat treatments ware designed for different cooling conditions. The salt bath was used to cooling as a medium with subsequent cooling on the water or in the air. The FEM method was used to designing the heat treatment conditions. The Johnson-Mehl-Avrami-Kolmogorov equation and the Koistinen-Marburger equations were used to prediction the microstructure phases. The microstructures were verified with experimental measurements. The ASTM G65 method was using for abrasion resistance tests. The results show that this procedure can be used to designing parameters of heat treatment of agricultural tools.

Key words: chisel, abrasive wear, microstructure of steel, hardness.

INTRODUCTION

Micro-ploughing (Stawicki et al., 2017), micro-cutting (Ryabov et al., 2016), micro-fatigue (Lin et al., 2008) and micro-cracking (Swain & Biswas, 2017) are abrasive wear mechanisms. Abrasive wear causes damage to the surface of agricultural tools and entrainment of material from the surface (Sidorov et al., 2017; Yazici & Çavdar, 2017). Worn agricultural tools are the cause of lower soil quality such as depth of processing, breadth of processing or soil mixing (Arvidsson & Bölenius, 2006; Manuwa, 2009). Abrasive wear causes a change in shape of the tool causing an increase in force on the tool and the entire machine (Kichler et al., 2011). The microstructure of the steel is important for the intensity of abrasive wear (Sabet et al., 2011; Votava 2014). The articles (Das Bakshi et al., 2013; Gola et al., 2017) state that the most suitable microstructure for abrasive wear is bainite and martensite. Soil resistance affects agricultural tools, so the tool's abrasion resistance is not enough, the toughness, strength

and hardness of the tool are also necessary (Votava et al., 2016; Ziemelis & Verdins, 2017).

Experimental tests would be too costly to find a suitable combination of toughness, strength and hardness of steel. The resulting microstructure and hardness can be predicted by mathematical models using finite element method (Serajzadeh, 2004; Teixeira et al., 2009). Heat flux (Babu & Prasanna Kumar, 2009; Prasanna Kumar, 2013), thermal conductivity and specific heat capacity (Telejko, 2004; Telejko & Malinowski, 2004) are important to build FEM models.

The phase transformation of austenite to martensite is non-diffusion process. Non-diffusion process can be described Koistinen-Marburger equations. Transformation of austenite to bainite, ferrite or pearlite is a diffusion process. The diffusion process can be described by Johnson-Mehl-Avrami-Kolmogorov equations (Martin, 2010; Wróbel et al., 2017).

Heat treatment of steels is important for the proportions of the individual phases of the resulting microstructure. Heat treatment in salt baths also called as isothermal hardening is a modern trend in steel processing. Isothermal quenching provides the possibility of setting conditions such as ambient temperature stability, higher cooling temperature required to create bainite, heat transfer from product to salt bath (Beck et al., 2015; Urbanec et al., 2015; Jaason et al., 2016).

The ASTM G65 method is a standardized method for comparing abrasion resistance. ASTM G65 defines the exact parameters of abrasion resistance tests, so results can be comparable to other steel tests (Elalem & Li, 1999; Doering et al., 2011; Hyttel et al., 2013).

The aim of this work is to design a model of microstructure distribution after heat treatment. The microstructure is verified with experimental measurements. Abrasion resistance tests were carried out on tested steels.

MATERIALS AND METHODS

25CrMo4 steel (steel no. 1.7218) has been chosen for this experiment. The chemical composition of the steel is shown in Table 1.

Table 1. Chemical composition of steel 25CrMo4 (wt.%)

Steel	C	Mn	Si	P	S	Cr	Ni	Cu	Al	Mo	Sn	V	Ti
25CrMo4	0.25	0.71	0.23	0.018	0.022	1.03	0.09	0.23	0.023	0.21	0.011	0.004	0.015

Experimental measuring:

Samples were made from a rod of Ø25 mm. The sample was adjusted to the dimensions 25 x 10 x 50 mm (according to the standard ASTM G65). The surfaces of the sample were ground with a diamond wheel. Struers MD Allegro was used with diamond suspension of 9 μm.

All samples were heated in air at 800 °C for 1,200 seconds. Sample cooling was carried out in combinations of the salt bath 50 wt.% $NaNO_2$ + 50 wt.% $NaNO_3$, water and air cooling media – see Table 2.

Table 2. Setting of heat treatment of steel samples

	1. cooling			2. cooling			3. cooling		
Sample [-]	Temp. [°C]	Medium [-]	Time [s]	Temp. [°C]	Medium [-]	Time [s]	Temp. [°C]	Medium [-]	Time [s]
1	400	salt bath	37	400	air	163	20	air	to 20 °C
2	400	salt bath	37	20	water	to 20 °C	-	-	-
3	400	salt bath	20	20	water	to 20 °C	-	-	-
4	400	salt bath	30	20	water	to 20 °C	-	-	-
5	400	salt bath	500	20	water	to 20 °C	-	-	-
6	20	water	to 20 °C	-	-	-	-	-	-

FEM model:

The heat flux was obtained by the procedure described in the work (Kešner et al., 2016). Specific heat capacity and thermal conductivity were obtained by the procedure which was described in (Kešner et al., 2017). Calculation of microstructure and hardness were obtained according to the algorithm shown in Fig. 3.

Steel time transitions are implemented in the model between different cooling media (salt bath 50 wt.% $NaNO_2$ + 50 wt.% $NaNO_3$, water and air). Time transitions are defined in the library software ElmerFem (CSC 2017). Heat flux of steel were used and temperature of cooling media, specific heat capacity and thermal conductivity as boundary conditions.

The model was sketched in 2D with a mapped mesh network with three points created from which the analysis of the resulting data is performed. Created points correspond to the placement of temperature sensors in a laboratory experiment. Point 2 is located 3 mm below the surface in the longitudinal direction, point 1 is located in the center of the longitudinal direction see Fig. 1.

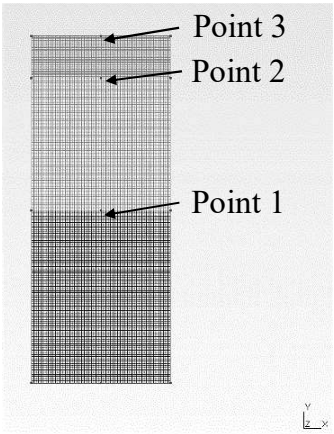

Figure 1. Mesh Network Model with Marked Points.

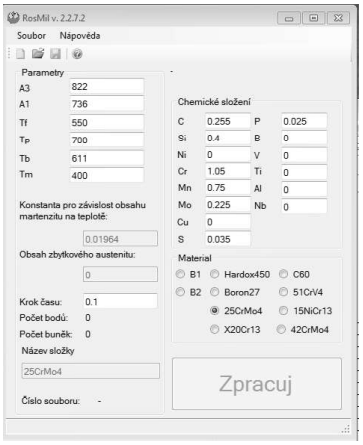

Figure 2. Software for calculating the volume of the phases.

Fig. 3 shows the flowchart of calculating the volume of the final phases and the hardness of the steel after heat treatment. MS Visual basic language (Microsoft 2010) was use for algorithm, which is show in Fig. 3. The software allows you to select the type of steel for analysis – see Fig. 2. The software allows you to select the type of steel for analysis (contains all the properties and constants of the steel to calculate Johnson-

Mehl-Avrami-Kolmogorov and Koistinen-Marburger equations). Johnson-Mehl-Avrami-Kolmogorov and Koistinen-Marburger equations have been taken from the articles (Kirkaldy, 2007; Sinha et al., 2007; Chotěborský & Linda, 2015). The parameters can be changing after selection of the steel.

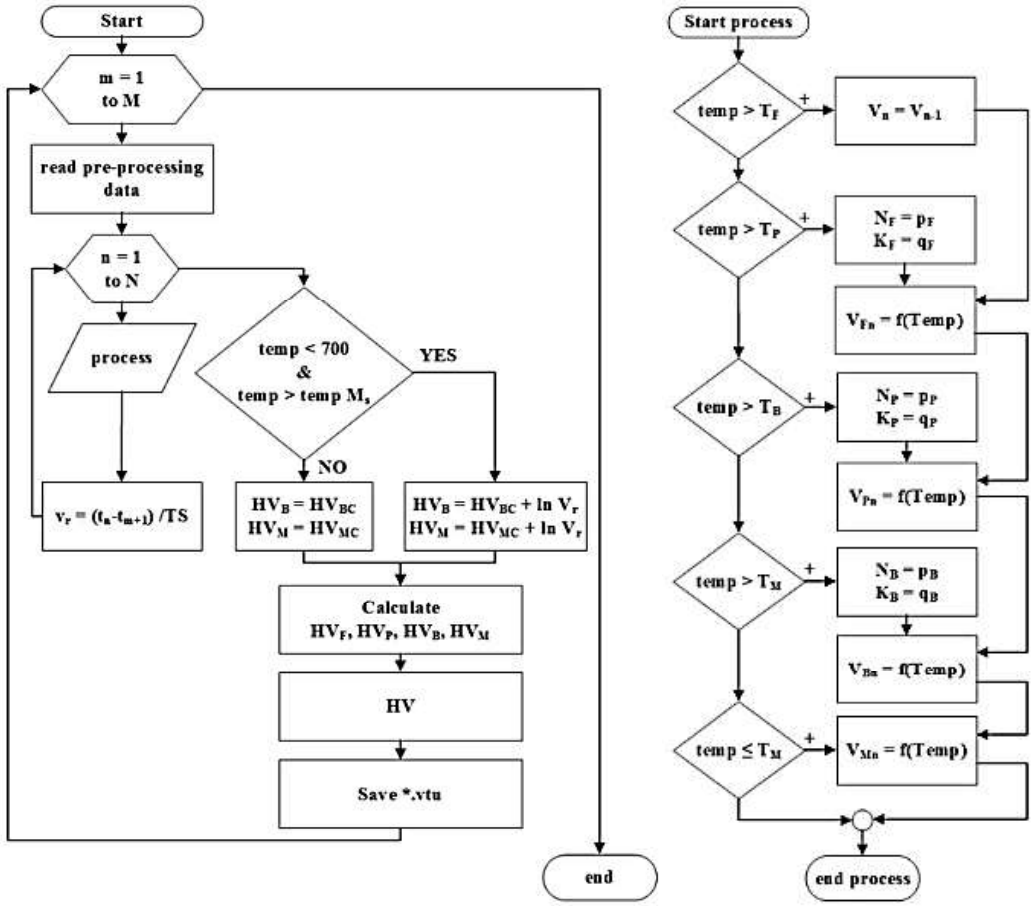

Figure 3. The flowchart of calculating the volume of the final phases and the hardness of the steel after heat treatment.

The calculation procedure use a data of the heat model from the ElmerFem finite element method, where the boundary conditions are present in the Table 2. The **.vtu* files of heat field are loaded to our MS VB.net algorithm, where *m* defines the current calculation step, the loaded input file and *M* defines the total number of input files. The temperature information processing is performed in individual nodes, *n* is the current node of calculation and *N* is the total number of nodes. In the 'process' subroutine, the individual parts of the calculation of volumetric concentrations of the ferrite, perlite, bainite, martensite phases according to the Johnson-Mehl-Avrami-Kolmogorov and Koistinen-Marburger equations were define. A condition for the calculation of the individual phases is always the achievement of the respective temperatures and the phase formation time according to the TTT and CCT diagrams. The cooling rate is included in

the calculation. The calculation of hardness starts after the completion of the calculation of the 'process' subroutine and the termination of the calculation loop of all nodes. The hardness is calculated according to the volume of the individual phases and then the total hardness is calculated. The resulting data and temperature are stored in a new **.vtu* file in the same xml format as the original data. Data processing is performed in the program ParaView (Sandia Corporation, 2015).

Fig. 4 shows the temperature gradient of sample 2 at 37 s, at the time of transition to another cooling media.

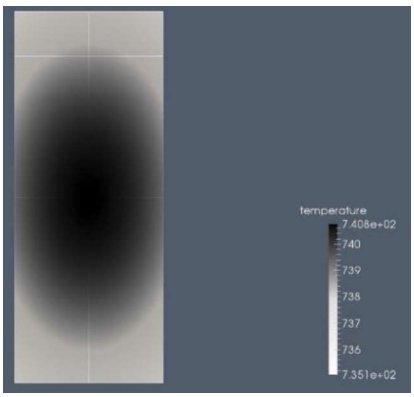

Figure 4. Temperature gradient for sample 2 at the time of 37 s.

Fig. 5 shows cooling of sample 2. The sample was cooled for 37 seconds in a salt bath (400 °C) and then transferred to air (20 °C). The temperature curves are presented for 3 points – Fig. 1. Point 1 is the border point of the model, hence its temperature falls below the set limit of 20 °C.

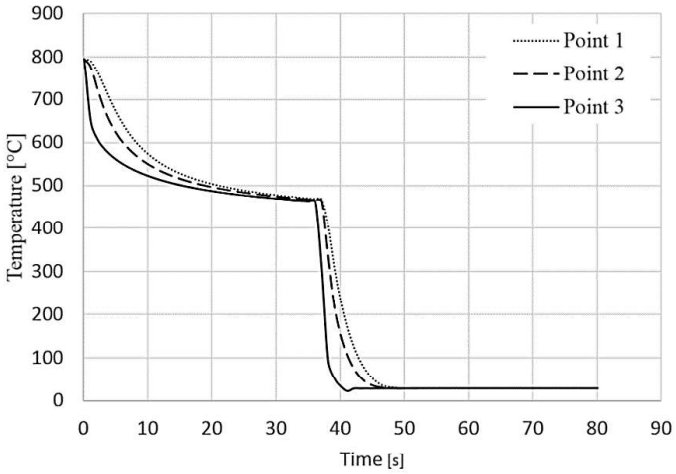

Figure 5. Cooling curves for sample 2.

RESULTS AND DISCUSSION

The microstructure phase volume at points 1, 2, 3 (location on the sample of Fig. 1) is shown in Figs 6–8. The difference was found between the microstructure of the ferrite as determined by the model and the experimentally measured microstructure of the ferrite, especially in models 1, 2 and 5 – shown Fig. 6. The difference of 36% is the largest for sample 1 in point 3. In point 1, the difference dropped to 15%. For sample 2, the greatest difference is 22% at point 2. The 32% difference in point 3 was found in sample 5.

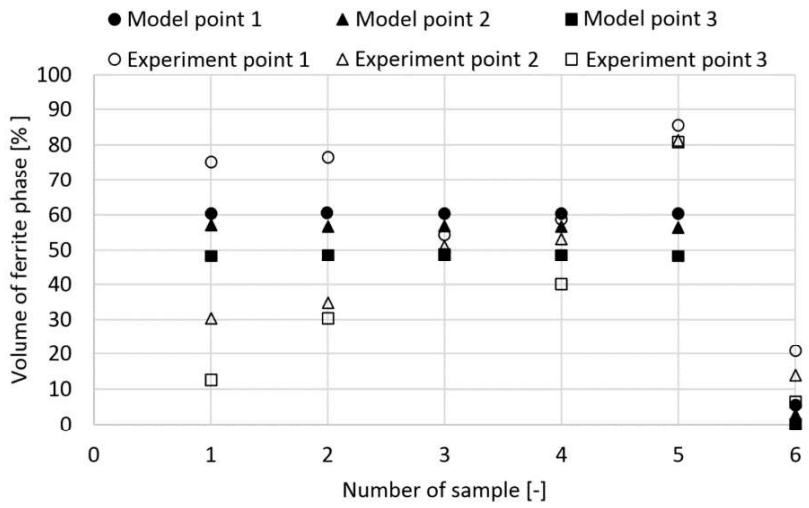

Figure 6. The volume of the ferrite phase in individual samples.

Differences in the bainite microstructure are visible as well as in the ferrite microstructure, ie in samples 1, 2 and 5 – shown Fig. 7. The greatest difference of 35% is measured on the sample is a 1 in the point 3 between the experimentally measured and calculated bainite. Sample 2 at point 3 has a difference of 20% of the microstructure. In point 1, the difference is reduced to 15%. A large difference of 33% was found for sample 5 – at point 3. Samples 3, 4 and 6 had the difference between microstructures measured and calculated by max. 15%.

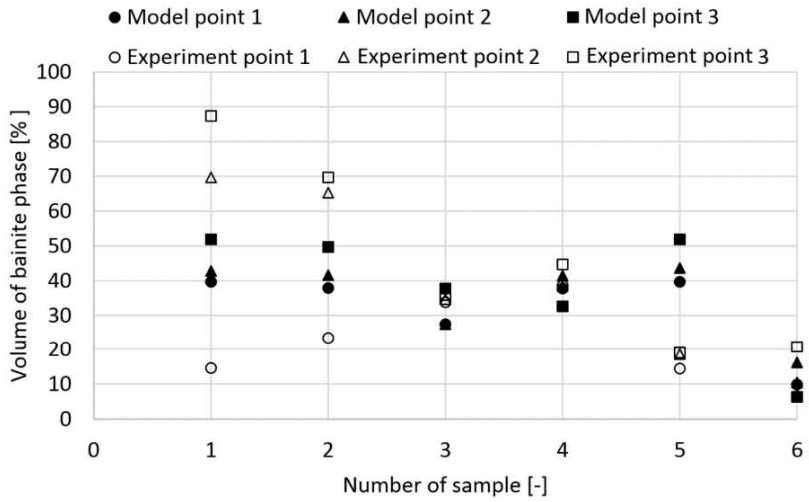

Figure 7. The volume of the bainite phase in individual samples.

The volume of martensite is considerably smaller relative to the microstructure of bainite and ferrite. The occurrence of martensite microstructure was not recorded in samples 1 and 5 – neither in the experimental part nor in the model part. Differences of 2% of the martensite microstructure were found for samples 1 to 5. The difference

volume of martensite in sample 6 was 21% in point 3. At point 2, the difference was significantly reduced to 5% and in point 1 it decreased to 12%.

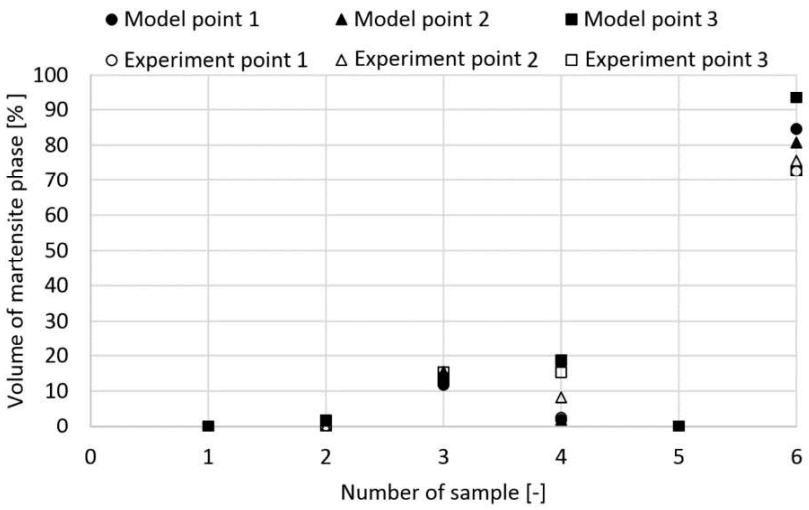

Figure 8. The volume of the martensite phase in individual samples.

Hardness of HV is shown in Fig. 9. Distribution of hardness for the model and the experiment is divided by points 1, 2, 3 (arrangement shown in Fig. 1). The differences are apparent in the samples 1 to 5. Different hardness values are due to the differences between phases between the experiment and the model. The hardness of sample 6 shows the difference in point 3. At point 3, the difference between the microstructure is described above.

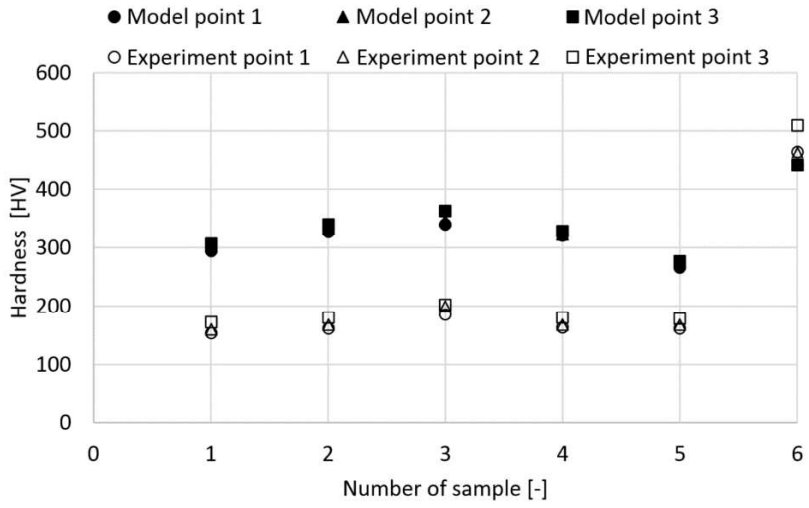

Figure 9. Hardness of HV in individual samples.

The Program Statistica 12 (StatSoft, 2014) was used for statistical evaluation. Dependence was evaluated between loss of weight on the microstructure of bainite,

martensite and ferrite. A weight loss of 1 meter was used for the calculation. Equation (1) was compiled to describe the ideal representation of the microstructure for the lowest abrasive wear.

$$\psi = 0.081 + 3.8 \cdot 10^{-6} \cdot V_F^2 + 1.18 \cdot 10^{-6} \cdot V_B^2 + 1.09 \cdot 10^{-6} \cdot V_M^2 \qquad (1)$$

where ψ – weight loss, %; V_F – volume of ferrite phase, %; V_B – volume of bainite phase, %; V_M – volume of martensite phase, %.

The results were evaluated in terms of the lowest weight loss. For the smallest weight loss it is advisable to use a structure that contains a maximum of 10% ferrite and bainite + martensite, each of which is in the range of 40% to 60%.

Specific heat capacity, thermal conductivity and heat flux was measured accurately for the steel 25CrMo4 – samples were prepared from the same rod. For this reason, it can be assumed that the differences found in microstructures between the experimental measurement and the model may be due to the assumed boundaries of the emergence of new phases from the TTT diagram. Border shift occurs when steel is alloyed with some elements such as chrome. The mathematical model then calculates the different beginnings of the boundaries of new phase phases, thus changing the microstructure distribution.

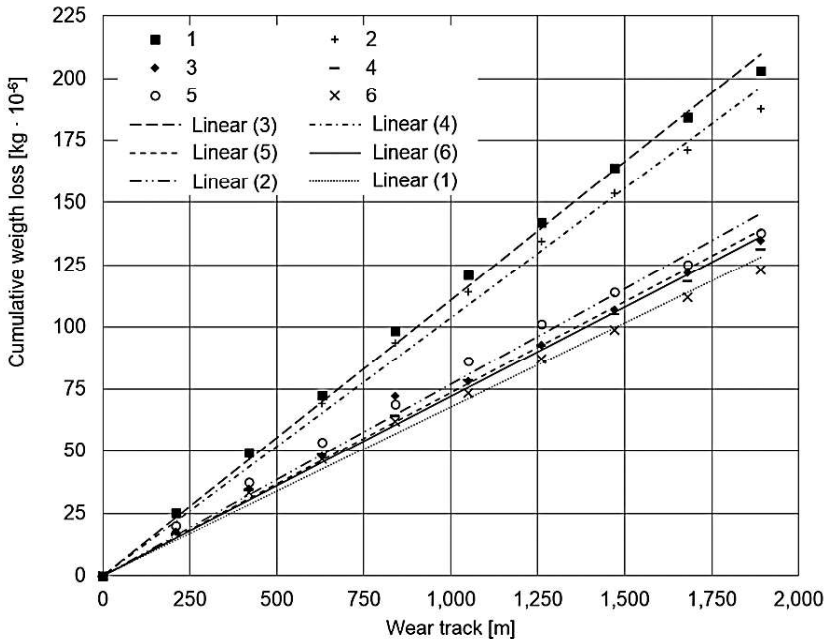

Figure 10. Abrasive wear depending on the cumulative loss of weight over the wear track (distance traveled by the disc).

The cumulative weight loss in relation to the path is shown in Fig. 10. Sample 1 and sample 2 have the least resistance to abrasive wear.

Samples 3 through 6 have significantly better abrasion resistance. The highest resistance to abrasion wear has a sample of 6. Sample 6 has a significantly greater volume of martensite (70%) than samples 1 to 5. At the same time there is a reduction

in the volume of ferrite – on the surface of the sample, where the test was conducted with ASTM G65 volume of ferrite is 12%. This value is similar to the statistical model (the proportion of ferrite to 12%). The volume between the structure of bainite and martensite is ideally fifty to fifty – in this case 44% bainite and 44% martensite. A sample experiment shown 72% volume of martensite on the surface for sample 6. For samples 1 to 5, the volume of ferrite is significantly higher – for these samples, abrasion resistance is reduced. This fact corresponds to the statistical model mentioned above.

The suitability of the bainite and martensite structure for abrasion resistance is described in the literature (Hernandez et al., 2016; Narayanaswamy et al., 2016; Trevisiol et al., 2017). This fact confirms the accuracy of the statistical model in terms of the mutual share of bainite, martensite and ferrite for resistance to abrasion wear.

Babu, Prasanna Kumar (2011) in their work, states that the magnitude of the heat flux is affected by the chemical composition of the steel. In this work the chemical composition was taken from the material sheet which was supplied with steel. The chemical composition, that has been inserted into the computational models, may have small deviations, that cause the change in the size of the heat flow. The amount of heat flow is related to the calculation of the phase volume after heat treatment. For this reason, the difference between the mathematical model and the experiment can vary by up to 36% for the phase volume calculation.

CONCLUSIONS

Various heat treatment was chosen for the steel 25CrMo4. The statistical model shows that the most appropriate distribution of the microstructure is up to 10% ferrite, and the martensite content with bainite is 40% to 60% – ideally divided by half. Differences between the experimentally measured and calculated microstructure were found to 35%. This difference may be due to addition of alloying elements in the steel, because the chemical composition of steel was taken from the material sheets supplied together with steel. The hardness for samples 1 through 5 was about 150 HV lower for the model than for the experiment. This fact is due to the accuracy of calculation of the microstructure. The procedure described in this paper could be used to predict the microstructure after heat treatment. Differences between the microstructure measured and the model microstructure can be reduced by refining the chemical composition of the steel.

ACKNOWLEDGEMENTS. Supported by Internal grant 31140/1312/3114 agency of Faculty of Engineering, Czech University of Life Sciences in Prague.

REFERENCES

CSC – IT Center for Science 2014. Elmer finite element software [online]. Available from: *http://www.csc.fi/english/pages/elmer*

Arvidsson, J. & Bölenius, E. 2006. Effects of soil water content during primary tillage – laser measurements of soil surface changes. *Soil and Tillage Research* **90**, 222–229.

Babu, K. & Prasanna Kumar, T.S. 2009. Mathematical Modeling of Surface Heat Flux During Quenching. *Metallurgical and Materials Transactions B* **41**, 214–224.

Babu, K. & Prasanna Kumar, T.S. 2011. Effect of CNT concentration and agitation on surface heat flux during quenching in CNT nanofluids. *International Journal of Heat and Mass Transfer* **54**, 106–117.

Beck, M., Schmidt, C., Ahrenberg, M., Schick, C., Kragl, U. & Kessler, O. 2015. Ionic Liquids as New Quenching Media for Aluminium Alloys and Steels. *HTM Journal of Heat Treatment and Materials* **70**, 73–80.

Das Bakshi, S., Shipway, P.H. & Bhadeshia, H.K.D.H. 2013. Three-body abrasive wear of fine pearlite, nanostructured bainite and martensite. *Wear* **308**, 46–53.

Doering, A., Danks, D., Mahmoud, S. & Scott, J. 2011. Evaluation of ASTM G65 abrasive - Spanning 13 years of sand. *Wear* **271**, 1252–1257.

Elalem, K. & Li, D.Y. 1999. Dynamical simulation of an abrasive wear process. *Journal of Computer-Aided Materials Design* **6**, 185–193.

Gola, A.M., Ghadamgahi, M. & Ooi, S.W. 2017. Microstructure evolution of carbide-free bainitic steels under abrasive wear conditions. *Wear* **376–377**, 975–982.

Hernandez, S., Leiro, A., Ripoll, M.R., Vuorinen, E., Sundin, K.G. & Prakash, B. 2016. High temperature three-body abrasive wear of 0.25C 1.42Si steel with carbide free bainitic (CFB) and martensitic microstructures. *Wear* **360–361**, 21–28.

Hyttel, M.W., Olsson, D.D., Reisel, G. & Bøttiger, J. 2013. Comparison of a newly developed compression-twist abrasive wear test with the ASTM G65 test method. *Wear* **307**, 134–141.

Chotěborský, R. & Linda, M. 2015. FEM based numerical simulation for heat treatment of the agricultural tools. *Agronomy Research* **13**, 629–638.

Jaason, K., Peetsalu, P., Kulu, P., Saarna, M. & Beilmann, J. 2016. Predictive tools for the isothermal hardening of strip steel parts in molten salt. *Proceedings of the Estonian Academy of Sciences* **65**, pp. 152–158.

Kešner, A., Chotěborský, R. & Linda, M. 2016. Determination of the heat flux of steel for the heat treatment model of agricultural tools. *Agronomy Research* **14**, 1004–1014.

Kešner, A., Chotěborský, R. & Linda, M. 2017. Determining the specific heat capacity and thermal conductivity for adjusting boundary conditions of FEM model. *Agronomy Research* **15**, 1033–1040.

Kichler, C.M., Fulton, J.P., Raper, R.L., Mcdonald, T.P. & Zech, W.C. 2011. Effects of transmission gear selection on tractor performance and fuel costs during deep tillage operations. *Soil and Tillage Research* **113**, 105–111.

Kirkaldy, J.S. 2007. Flux-independent theory of nonlinear diffusion for Vegard's law solutions. *Materials Science and Engineering: A*. **444**, 104–111.

Lin, Y.J., Agrawal, A. & Fang, Y. 2008. Wear progressions and tool life enhancement with AlCrN coated inserts in high-speed dry and wet steel lathing. *Wear* **264**, 226–234.

Manuwa, S.I. 2009. Performance evaluation of tillage tines operating under different depths in a sandy clay loam soil. *Soil and Tillage Research* **103**, 399–405.

Martin, D. 2010. Application of Kolmogorov–Johnson–Mehl–Avrami equations to non-isothermal conditions. *Computational Materials Science* **47**, 796–800.

Microsoft. Visual Basic . NET. 2010

Narayanaswamy, B., Hodgson, P., Timokhina, I. & Beladi, H. 2016. The Impact of Retained Austenite Characteristics on the Two-Body Abrasive Wear Behavior of Ultrahigh Strength Bainitic Steels. *Metallurgical and Materials Transactions A* **47**, 4883–4895.

Prasanna Kumar, T.S. 2013. Influence of Steel Grade on Surface Cooling Rates and Heat Flux during Quenching. *Journal of Materials Engineering and Performance* **22**, 1848–1854.

Ryabov, V.V., Motovilina, G.D., Khlusova, E.I., Sidorov, S.A. & Khoroshenkov, V.K. 2016. Study of the Structure of New Wear-Resistant Steels for Agricultural Machinery Components After Operational Tests. *Metallurgist* **60**, 839–844.

Sabet, H., Khierandish, Sh., Mirdamadi, Sh. & Goodarzi, M. 2011. The Microstructure and Abrasive Wear Resistance of Fe–Cr–C Hardfacing Alloys with the Composition of Hypoeutectic, Eutectic, and Hypereutectic at Cr. C. ¼ 6. H. *Tribology Letters* **44**, 237–245.

Sandia Corporation, Kitware Inc, 2015. *ParaView 4.3.1* [online]. 2015. New Mexico PO Box 5800 Albuquerque, NM 87185: Sandia Corporation, Kitware Inc. Available from: www.paraview.org

Serajzadeh, S. 2004. A mathematical model for prediction of austenite phase transformation. *Materials Letters* **58**, 1597–1601.

Sidorov, S.A., Khoroshenkov, V.K., Lobachevskii, Ya.P. & Akhmedova, T.Sh. 2017. Improving Wear Resistance of Agricultural Machine Components by Applying Hard-Alloy Thick-Layer Coatings Using Plasma Surfacing. *Metallurgist* **60**, 1290–1294.

Sinha, V.K., Prasad, R.S., Mandal, A. & Maity, J. 2007. A Mathematical Model to Predict Microstructure of Heat-Treated Steel. *Journal of Materials Engineering and Performance* **16**, 461–469.

Statsoft. 2014. Statistica [online]. 2014. Available from: http://www.statsoft.com/

Stawicki, T., Białobrzeska, B. & Kostencki, P. 2017. Tribological Properties of Plough Shares Made of Pearlitic and Martensitic Steels. *Metals* **7**, 139–158.

Swain, P.T.R. & Biswas, S. 2017. Abrasive Wear Behaviour of Surface Modified Jute Fiber Reinforced Epoxy Composites. *Materials Research* **20**, 661–674.

Teixeira, M.G., Rincon, M.A. & Liu, I.-S. 2009. Numerical analysis of quenching – Heat conduction in metallic materials. *Applied Mathematical Modelling* **33**, 2464–2473.

Telejko, T. & Malinowski, Z. 2004. Application of an inverse solution to the thermal conductivity identification using the finite element method. *Journal of Materials Processing Technology* **146**, 145–155.

Telejko, T. 2004. Analysis of an inverse method of simultaneous determination of thermal conductivity and heat of phase transformation in steels. *Journal of Materials Processing Technology* **155–156**, 1317–1323.

Trevisiol, C., Jourani, A. & Bouvier, S. 2017. Effect of hardness, microstructure, normal load and abrasive size on friction and on wear behaviour of 35NCD16 steel. *Wear* **388–389**, 101–111.

Urbanec, J., Saastamoinen, A., Kivivuori, S. & Louhenkilpi, S. 2015. Fast Salt Bath Heat Treatment for a Bainitic/Martensitic Low-Carbon Low-Alloyed Steel. *Metallurgical and Materials Transactions A*. **46**, 5343–5349.

Votava, J. 2014. Usage of abrasion-resistant materials in agriculture. *Journal of Central European Agriculture* **15**, 119–128.

Votava, J., Kumbár, V. & Polcar, A. 2016. Optimisation of Heat Treatment for Steel Stressed by Abrasive Erosive Degradation. *Acta Universitatis Agriculturae et Silviculturae Mendelianae Brunensis* **64**, pp. 1267–1277.

Wróbel, J., Kulawik, A. & Bokota, A. 2017. The Numerical Analysis of the Hardening Phenomena of the Hot-work Tool Steel. *Procedia Engineering* **177**, 33–40.

Yazici, A. & Çavdar, U. 2017. A Study of Soil Tillage Tools from Boronized Sintered Iron. *Metal Science and Heat Treatment* **58**, 753–757.

Ziemelis, M. & Verdins, G. 2017. Plough parts wear resistance depending on their material composition and processing technology. *Engineering for Rural Development* **16**, 455–460.